Journal of Engineering Mathematics 18 (1984) 133–156


# The response of a confined gas to a thermal disturbance: rapid boundary heating

A.M. RADHWAN *

*Mechanical Engineering Department, University of Colorado, Boulder, CO 80309, USA*

D.R. KASSOY **

*School of Mathematics and Physics, University of East Anglia, Norwich NR4 7TJ, England*

(Received September 27, 1983)

## Summary

An inert compressible gas confined between infinite parallel planar walls is subjected to significant heat addition at the boundaries. The wall temperature is increased during an interval which is scaled by the acoustic time of the container, defined as the passage time of an acoustic wave across the slab. On this time scale heat transfer to the gas occurs in thin conductive boundary layers adjacent to the walls. Temperature increases in these layers cause the gas to expand such that a finite velocity exists at the boundary-layer edge. This mechanical effect, which is like a time-varying piston motion, induces a planar linear acoustic field in the basically adiabatic core of the slab. A spatially homogeneous pressure rise and a bulk velocity field evolve in the core as the result of repeated passage of weak compression waves through the gas. Eventually the thickness of the conduction boundary layers is a significant fraction of the slab width. This occurs on the condition time scale of the slab which is typically a factor of $10^6$ larger than the acoustic time. The further evolution of the thermomechanical response of the gas is dominated by a conductive–convective balance throughout the slab. The evolving spatially-dependent temperature distribution is affected by the homogeneous pressure rise (compressive heating) and by the deformation process occurring in the confined gas. Superimposed on this relatively slowly-varying conduction-dominated field is an acoustic field which is the descendent of that generated on the shorter time scale. The short-time-scale acoustic waves are distorted as they propagate through a slowly-varying inhomogeneous gas in a finite space. Solutions are developed in terms of asymptotic expansions valid when the ratio of the acoustic to conduction time scales is small. The results provide an explicit expression for the piston analogy of boundary heat addition.

## 1. Introduction

When energy is added to a compressible gas at a boundary or within the material itself one can expect to observe a mechanical response. The temperature rise associated with heat addition causes a localized gas-expansion process which in turn can generate acoustic effects. Lord Rayleigh [1] provided an early account of acoustic wave generation in a confined gas due to a small impulsive increase in boundary temperature. A linearized energy equation was derived by assuming that disturbances were small and that the transient pressure response was spatially homogeneous. Better modelling of the interaction

* Permanent address: Mechanical Engineering Department, King Abdulaziz University, Jeddah, Saudi Arabia.
** Permanent address: Mechanical Engineering Department, University of Colorado, Boulder, CO 80309, USA.

between slow conduction-dominated thermal effects and the much faster acoustic mechanical processes requires a systematic examination of the complete equations for a viscous, heat-conducting compressible gas. Wu [2] studied linear disturbances generated in a gas by distributed sources of energy and/or forces. He demonstrated that a small conduction-dominated region would form around an impulsive concentrated heat source. Acoustic waves are generated a short time later by the localized gas expansion. There is a conceptual limitation in Wu's theory because heat is added instantaneously relative to a characteristic time $\tau_0$ which is in fact the mean time between molecular collisions. This can be accomplished only with a radiative source. Subsequent gas expansion can occur only after many multiples of $\tau_0$ have elapsed during which heat added at the source is conducted (a result of many energy exchanging molecular collisions) into a localized neighbouring volume of material. In this sense Wu's solutions for times less than $\tau_0$ have no physical meaning.

Trilling [3] described the character of a linear acoustic field in a semi-infinite space induced by a small impulsive temperature increase at the origin. The complete linearized equations are used in the mathematical model. Here again the spatial dimension and the time are scaled with respect to the mean free path and collision time respectively, while the boundary-temperature rise is instantaneous on the latter scale. As a result, the short-time solution, which is supposed to describe the conduction-dominated heat transfer adjacent to the boundary, is of questionable validity because the interval is too limited for energy exchange by collisions. Related studies, emphasizing the effects of conductivity and viscosity on acoustic wave propagation, have been carried out by Knudsen [4] and by Luikov and Berkoresky [5].

Pressure waves generated by a heat source in an inviscid, nonconducting gas were considered by Chu [6]. The actual mechanism of wave generation is absent, because conductive energy transport is not available to heat up a local volume of gas leading to bulk expansion. Rather, Chu derives a formal statement relating the heat addition to an effective piston speed. This piston analogy is then used to construct a linear theory of wave propagation valid for small piston Mach numbers. In physical terms this limitation requires that the energy addition per unit mass be small compared to the initial thermal energy in the region of interest. Shock-wave generation associated with more significant continuous heat addition is also considered.

Larkin [7], Thuraisamy [8], Spradley et al. [9] and Spradley and Churchill [10] have computed the gas motion induced in a slab-like container when the temperature on one-boundary is raised impulsively while the other is held at the initial temperature of the system. The general nonlinear conservation equations, ignoring viscous dissipation, are used as the basis of the study. The numerical solutions resolve the passage of acoustic waves across the slab during the early phase of the process. Larkin and Thuraisamy find wave amplitudes ten times larger than Spradley et al. which the latter attribute to unspecified numerical difficulties. The difficulty probably occurs because the spatial resolution used is not fine enough to resolve the conduction-dominated boundary layer adjacent to the heated wall on the acoustic time scale of the slab. If the gas expansion process in the boundary layer is not described accurately then the acoustic waves generated will be equally in error. For larger values of the time (measured with respect to the acoustic passage time across the slab) the pressure is found to be a spatially homogeneous increasing function of time. The effect of bulk motion induced into the gas by repeated passage of acoustic waves is to speed the approach to an equilibrium temperature distribution relative to that in a rigid conducting material. It is difficult to assess the accuracy of these solutions because it is unclear if the numerical methods have resolved both the diffusive thermal processes and the wave-like acoustic effects occuring at the same time.

Kassoy [11] has calculated the response of an inert perfect gas confined in a slab to a boundary-temperature increase occurring over the conduction-time scale $t'_c$ of the container. The earliest phase of the process takes place on the acoustic time scale $t'_A$, where $t'_A = O(10^{-6}\, t'_c)$. Thin conductive boundary layers appear adjacent to each wall where the temperature rises continuously, although the change in size is small. The expanding gas in the boundary layer acts like an effective piston, driving linear compressive waves into the core of the slab. Repeated passage of the continuously generated acoustic field causes a small bulk velocity and a spatially homogeneous compression to develop. Eventually the time becomes large relative to $t'_A$ and conductive effects spread into the interior of the slab. The subsequent heat-transfer process develops on the scale of $t'_c$. During this longer period the bulk gas velocity is small but must be retained in the basic nonlinear mass-conservation and energy equations. Superimposed on the slowly-varying conduction-dominated solutions, the previously generated acoustic waves continue to evolve in a linear fashion. As they propagate through the inhomogeneous (variable-temperature) material, they prevent the development of any spatial pressure gradients. As a result the spatially homogeneous pressure increase can be calculated in terms of a spatial integral of the temperature distribution. These conceptual arguments are developed from a systematic study of distinguished limits of the complete Navier-Stokes equations based on an asymptotic analysis when $t'_A/t'_c \ll O(1)$. Numerical solutions for the conduction-dominated heat transfer process are given by Radhwan [12].

There are a variety of fascinating related thermoacoustic phenomena that occur in interior and exterior flows and which frequently play a role in noise generation. Some of the literature is described in [11] and [12] and in the monograph article by Rott [13]. In addition Vincenti and Traugott [14] have described the mechanical response of a gas to radiative heat transfer.

In the present work, the concepts developed in [11] are employed to study the mechanical response of a gas in a slab when boundary heating occurs on the acoustic-time scale of the container. During that period the energy addition at the boundary is $O(10^6)$ larger than that considered in [11]. As a result the acoustic field generated by the boundary-layer gas expansion is a similar factor larger. In fact the velocity field associated with the acoustic process is a factor of $10^3$ larger than that associated with bulk gas deformation during the longer conduction-dominated process. The acoustic field retains its linear character because the power added at the boundary is not large enough to drive an acoustic wave front which becomes nonlinear within the finite dimension of the slab. Numerical solutions for the nonlinear heat-transfer process, which includes gas deformation, are obtained to show how the system relaxes to the final steady state. Flow reversal is observed as density variations are smoothed out.

## 2. Mathematical model

The mathematical model must be capable of describing the thermomechanical response of a perfect gas confined in a slab to a wall temperature disturbance occuring on the acoustic time scale of the container, see Fig. 1. The slab walls are assumed to be conducting and rigid and the spacing between them is $L'$ (primes denote dimensional quantities). The gas

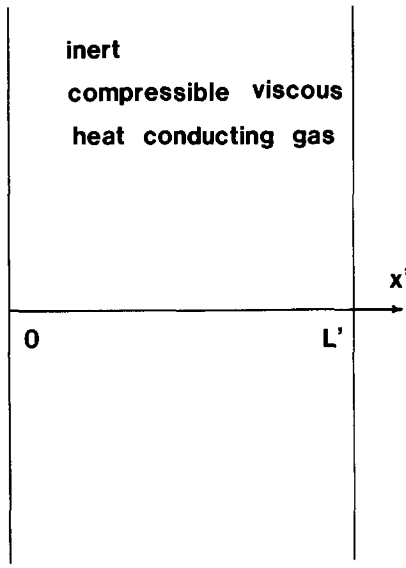


Figure 1. The geometrical configuration of the slab-shaped container.

is initially at rest and in an equilibrium thermodynamic state defined by the pressure $p_0'$, the density, $\rho_0'$ and temperature $T_0'$. The conduction time scale is defined as $t_c' = L'^2/\kappa_0'$ where $\kappa_0'$ is the thermal diffusivity of the gas in the reference state. The acoustic time scale is $t_A' = L'/C_0'$, where $C_0' = (\gamma R T_0')^{1/2}$ is the speed of sound, $\gamma$ is the constant ratio of specific heats and $R$ is the gas constant. The small perturbation parameter is $\epsilon = t_A' \, \mathrm{Pr}/t_c'$ where Pr is the Prandtl number of the initial state.

The dimensionless equations for a compressible, viscous, conducting, inert, perfect gas can be written [11] as

$$\rho_t + (\rho u)_x = 0, \tag{1}$$

$$p = \rho T, \tag{2}$$

$$\rho(u_t + u u_x) = -\gamma^{-1} p_x + \epsilon(4/3)(\mu u_x)_x, \tag{3}$$

$$\frac{\rho C_v}{(\gamma - 1)}(T_t + u T_x) = -p u_x + \epsilon\left[\frac{\gamma}{(\gamma - 1)\mathrm{Pr}}(k T_x)_x + (4/3)\gamma\mu(u_x)^2\right] \tag{4}$$

where the subscripts $t$ and $x$ denote partial derivatives and

$$\rho = \rho'/\rho_0', \qquad p = p'/p_0', \qquad T = T'/T_0', \qquad u = u/C_0',$$

$$t = t'/t_A', \qquad x = x'/L', \tag{5}$$

$$\mu = \mu'/\mu_0', \qquad C_v = C_v'/C_{v_0}', \qquad k = k'/k_0' \tag{6}$$

The viscosity, specific heat at constant volume and thermal conductivity

$$\mu = \mu(T), \qquad C_v = C_v(T), \qquad k = k(T), \tag{7}$$

respectively are arbitrary functions of temperature. The equilibrium initial conditions are

$$t=0; \qquad T=\rho=p=1, \qquad u=0, \qquad 0\leqslant x\leqslant 1. \tag{8}$$

The wall temperature is assumed to increase on the acoustic-time scale and the normal velocity there is zero:

$$x=0,1; \qquad T=1+Q(t), \qquad u=0, \qquad t\geqslant 0. \tag{9}$$

Here $\mathrm{d}Q/\mathrm{d}t=\mathrm{O}(1)$ and $Q(0)=0$. The solutions are found in terms of asymptotic expansions based on the limit $\epsilon\to 0$.

## 3. Acoustic-time solutions

The wall temperature is raised by an O(1) amount during an interval measured by the acoustic time scale. Only a thin layer of gas adjacent to the boundary will be affected by conductive heat transfer. Beyond that conductive region disturbances can arise only from mechanical coupling with the heated, expanding gas next to the wall. In order to model these conceptual ideas solutions must be developed in a thin conductive boundary layer and in a nearly isentropic core.

### *3a. The boundary layer*

As a result of the O(1) wall temperature change there will be a similar spatial variation across the boundary layer. The boundary-layer variables near $x=0$ can be written as

$$T=\tilde{T}, \qquad \rho=\tilde{\rho}, \qquad p=\tilde{p}, \qquad x=\epsilon^{1/2}z, \qquad u=\epsilon^{1/2}\tilde{u} \tag{10}$$

where the scalings have been chosen to produce a balance of conductive and convective energy transport. Then (1)–(4) become

$$\tilde{\rho}_t+(\tilde{\rho}\tilde{u})_z=0, \tag{11}$$

$$\tilde{p}=\tilde{\rho}\tilde{T}, \tag{12}$$

$$\epsilon\tilde{\rho}(\tilde{u}_t+\tilde{u}\tilde{u}_z)=-\gamma^{-1}\tilde{p}_z+\epsilon\tfrac{4}{3}(\mu\tilde{u}_z)_z, \tag{13}$$

$$\frac{\tilde{\rho}C_v}{(\gamma-1)}(\tilde{T}_t+\tilde{u}\tilde{T}_z)=-\tilde{p}\tilde{u}_z+\frac{\gamma}{(\gamma-1)\,\mathrm{Pr}}(k\tilde{T}_z)_z+\epsilon\tfrac{4}{3}\gamma\mu(\tilde{u}_z)^2. \tag{14}$$

A simpler form of this system, obtained by employing the Lagrangian transformation

$$y=\int_0^z\tilde{\rho}(s,t)\,\mathrm{d}s, \tag{15}$$

can be written as

$$\tilde{\rho}_t = (\tilde{\rho})^2 \tilde{u}_y = 0, \tag{16}$$

$$\tilde{p} = \tilde{\rho}\tilde{T}, \tag{17}$$

$$\epsilon\tilde{u}_t = -\gamma^{-1}\tilde{p}_y = \epsilon\tfrac{4}{3}(\mu\tilde{\rho}\tilde{u}_y)_y, . \tag{18}$$

$$\frac{C_v}{(\gamma-1)}\tilde{T}_t = -\tilde{p}\tilde{u}_y + \frac{\gamma}{(\gamma-1)\,\mathrm{Pr}}(k\tilde{\rho}\tilde{T}_y)_y + \epsilon\tfrac{4}{3}\gamma\mu\tilde{\rho}(\tilde{u}_y)^2. \tag{19}$$

In the limit $\epsilon \to 0$, the momentum equation (18) implies

$$\tilde{p} = P(t) + \epsilon\tilde{p}_0(t, y) + \ldots . \tag{20}$$

Then the lowest-order (subscript 0) approximate system describing the temperature, density, pressure and velocity fields is

$$\tilde{\rho}_{0_t} + (\tilde{\rho}_0)^2 \tilde{u}_{0_y} = 0, \tag{21}$$

$$P(t) = \tilde{\rho}_0\tilde{T}_0, \tag{22}$$

$$\tilde{u}_{0_t} = -\frac{1}{\gamma}\tilde{p}_{0_y} + \tfrac{4}{3}(\mu\tilde{\rho}_0\tilde{u}_{0_y})_y, \tag{13}$$

$$\frac{C_v}{(\gamma-1)}\tilde{T}_{0_t} = -P(t)\tilde{u}_{0_y} + \frac{\gamma}{(\gamma-1)\,\mathrm{Pr}}(k\tilde{\rho}_0\tilde{T}_{0_y})_y. \tag{24}$$

The initial, boundary and matching conditions are

$$t = 0; \qquad \tilde{T}_0 = \tilde{\rho}_0 = \tilde{p}_0 = 1, \qquad \tilde{u}_0 = 0, \tag{25}$$

$$y = 0; \qquad \tilde{T}_0 = 1 + Q(t), \qquad \tilde{u}_0 = 0, \qquad t \geqslant 0, \tag{26}$$

$$y \to \infty; \qquad \tilde{T}_0 = 1. \tag{27}$$

In order to proceed the spatially homogeneous function $P(t)$ must be found by considering the nature of the solution in the interior core of the gas.

### *3b. The core*

Heat addition at the wall causes the boundary-layer gas to expand into the container with a speed of $O(\epsilon^{1/2})$ as given in (10). The outer edge of the expanding boundary layer acts like a variable-speed piston, thus generating a similar mechanical disturbance in the core. It follows that the appropriate scaling transformations for velocity, density, temperature and pressure are

$$\hat{u} = \tilde{u}, \qquad \rho = 1 + \epsilon^{1/2}\hat{\rho}, \qquad T = 1 + \epsilon^{1/2}\hat{T}, \qquad p = P(t) + \epsilon^{1/2}\hat{p}. \tag{28}$$

These transformations can be used in (1)–(4) to show that

$$P(t) = 1. \tag{29}$$

During the acoustic period the pressure is basically the initial value with a small superimposed disturbance due to the mechanical effect of the expanding boundary layer. The core disturbances should be compared with the $O(\epsilon^{3/2})$ corrections found in the slow heating case in [11].

If (28) and (29) are used in (1)–(4), and the limit $\epsilon \to 0.$ is applied, then the basic approximations for the disturbance variables are described by

$$\hat{\rho}_{0_t} + \hat{u}_{0_x} = 0, \tag{30}$$

$$\hat{p}_0 = \hat{T}_0 + \hat{\rho}_0, \tag{31}$$

$$\gamma \hat{u}_{0_t} + \hat{p}_{0_x} = 0, \tag{32}$$

$$\hat{T}_{0_t} + (\gamma - 1)\hat{u}_{0_x} = 0. \tag{33}$$

A Taylor-series expansion for $C_v = C_v(T)$ where $T = 1 + \epsilon^{1/2}\hat{T}$ has been used to show that $C_v \sim 1 + O(\epsilon^{1/2})$. An appropriate combination of (30)–(33) yields equations describing isentropic linear acoustic wave propagation in the interior core region. For example the velocity field is described by

$$\hat{u}_{0_{tt}} = \hat{u}_{0_{xx}}. \tag{34}$$

The initial conditions are

$$t = 0; \qquad \hat{u}_0 = \hat{u}_{0_t} = 0. \tag{35}$$

The latter is derived from the initial condition on the pressure and from the momentum equation (32). The boundary conditions will be derived from the matching condition with the boundary-layer solution. It is necessary at this point to return to the boundary-layer equations and to develop an appropriate solution.

### *3c. The boundary-layer solution*

The boundary-layer equations (23) and (24) can be simplified further by using physically reasonable constitutive relations for viscosity and thermal conductivity, $\mu = k = T$, and by assuming for convenience that $C_v = 1$. Then if (22) and (29) are used in the resulting momentum and energy equations it can be shown that,

$$\tilde{u}_{0_t} = -\gamma^{-1}\tilde{p}_{0_y} + \tfrac{4}{3}\tilde{u}_{0_{yy}}, \tag{36}$$

$$\tilde{T}_{0_t} = -(\gamma - 1)\tilde{u}_{0_y} + \frac{\gamma}{\Pr}\tilde{T}_{0_{yy}}. \tag{37}$$

The appropriate initial, boundary and matching conditions are given in (25)–(27). The equation describing heat transfer in the boundary-layer region, derived by combining (21), $\tilde{\rho}_0\tilde{T}_0 = 1$, (36) and (37), has the elementary form,

$$\tilde{T}_{0_t} = \frac{1}{\Pr}\tilde{T}_{0_{yy}}. \tag{38}$$

If one writes for convenience $\tilde{T}_0 = 1 + \theta$,.(38) can be written as

$$\theta_t = \frac{1}{\Pr}\theta_{yy}. \tag{39}$$

The appropriate initial, boundary and matching conditions, derived from (25)–(27) are

$$t=0; \quad \theta = 0, \tag{40}$$

$$y=0; \quad \theta = Q(t) \quad t \geqslant 0, \tag{41}$$

$$y \to \infty; \quad \theta = 0 \quad t \geqslant 0. \tag{42}$$

The prescribed wall-temperature function $Q(t)$ will produce an O(1) change in $\theta$ for proportional variations in $t$ if $Q(t) = \mathrm{O}(1)$, i.e., an order-one change in temperature $\theta$ on the acoustic-time scale.

The solution of (39)–(42), calculated by Duhamel's theorem (Carslaw and Jaeger [15]), can be written as

$$\theta(\eta, t) = \frac{2}{\sqrt{\pi}}\int_\eta^\infty Q\left(t + \frac{y^2 \Pr}{4\xi^2}\right)\exp(-\xi^2)\mathrm{d}\xi \tag{43}$$

where

$$\xi = \frac{y}{2}\left[\frac{\Pr}{t-\lambda}\right]^{1/2}, \qquad \eta = \frac{y}{2}\left(\frac{\Pr}{t}\right)^{1/2}. \tag{44}$$

The velocity equation in the boundary layer is derived by combining the mass-conservation equation (21) with the state equation $\tilde{\rho}_0\tilde{T}_0 = 1$ to find

$$\tilde{u}_{0_y} = \tilde{T}_{0_t}, \qquad \tilde{u}_0(0, t) = 0 \tag{45}$$

where $\tilde{T}_0 = 1 + \theta$ and the boundary condition is found from (26). If (38) is used to replace the temperature-time derivative, then the velocity solution can be expressed as

$$\tilde{u}_0 = \frac{1}{\Pr}\left(\tilde{T}_{0_y}(y, t) - \tilde{T}_{0_y}(0, t)\right). \tag{46}$$

Far from the wall $T_{0_y}(y \to \infty, t) \to 0$ so that the fluid velocity is given by

$$\tilde{u}_0(y \to \infty, t) = -\frac{1}{\Pr}\tilde{T}_{0_y}(0, t). \tag{47}$$

It is the boundary heat flux which determines the general character of the fluid motion at the edge of the boundary layer. Equation (47) represents the most explicit statement possible for the piston analogy of boundary heat transfer [6].

A specific calculation is carried out for the wall temperature function

$$Q(t) = \begin{cases} Ct, & t < t_0 \\ Ct_0, & t \geqslant t_0 \end{cases}, \; t \geqslant 0, \tag{48}$$

where $C$ is a specified constant representing the rate of temperature increase and $t_0$ is a given cut-off time. The solution for $\theta$, obtained for this special function from (43), can be used to write the nondimensional temperature distribution as

$$\tilde{T}_0 = 1 + Ct\left[(1+2\eta^2)\operatorname{erfc}(\eta) - 2(\pi)^{-1/2}\eta\exp(-\eta^2)\right], \qquad t < t_0, \tag{49}$$

and,

$$\begin{aligned} \tilde{T}_0 = {} & 1 + Ct(1+2\eta^2)\left[\operatorname{erfc}(\eta) - \operatorname{erfc}\left(\eta/(1-t_0/t)^{1/2}\right)\right] \\ & + Ct_0 \operatorname{erfc}\left(\eta/(1-t_0/t)^{1/2}\right) \\ & + 2Ct(\pi)^{-1/2}\eta\left\{(1-t_0/t)^{1/2}\exp\left[-\eta^2/(1-t_0/t)\right]\right. \\ & \left. - \exp(-\eta^2)\right\}, \qquad t \geqslant t_0, \end{aligned} \tag{50}$$

where $\eta$ is given in (44) and erfc( ) is the complementary error function [16].

Equations (49) and (50) can be used in (46) to find the boundary-layer velocity field

$$\tilde{u}_0(\eta, t) = 2C\left(\frac{t}{\Pr}\right)^{1/2}\left\{\eta\operatorname{erfc}(\eta) + (\pi)^{-1/2}\left[1 - \exp(-\eta^2)\right]\right\}, \qquad t < t_0, \tag{51}$$

$$\begin{aligned} \tilde{u}_0(\eta, t) = 2C\left(\frac{t}{\Pr}\right)^{1/2} & \left\{\eta\left[\operatorname{erfc}(\eta) - \operatorname{erfc}\left(\eta/(1-t_0/t)^{1/2}\right)\right]\right. \\ & + (\pi)^{-1/2}\left[(1-t_0/t)^{1/2}\exp\left(-\eta^2/(1-t_0/t)\right) - \exp(-\eta^2)\right] \\ & \left. + (\pi)^{-1/2}\left[1 - (1-t_0/t)^{1/2}\right]\right\}, \qquad t \geqslant t_0. \end{aligned} \tag{52}$$

The velocity profile has the interesting property that

$$\lim_{\eta\to\infty} \tilde{u}_0 = K_1 t^{1/2}, \qquad t < t_0, \tag{53}$$

$$\lim_{\eta\to\infty} \tilde{u}_0 = K_1\left[t^{1/2} - (t-t_0)^{1/2}\right], \qquad t \geqslant t_0, \tag{54}$$

where

$$K_1 = 2C/(\pi \Pr)^{1/2} \tag{55}$$

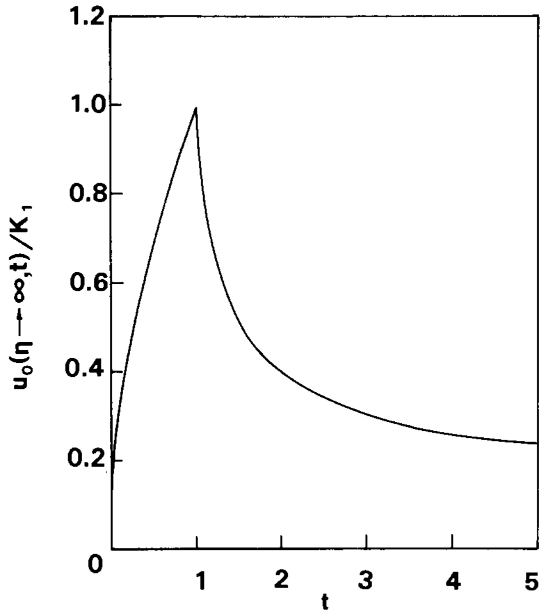


Figure 2. The time history of the speed $\hat{U}_0/K_1$ at the boundary-layer edge ($\eta \to \infty$) when $t_0 = 1$.

which can be interpreted to mean that for $t < t_0$, the thermal expansion of the gas results in a continuously accelerating piston-like effect at the edge of the boundary layer as shown in Fig. 2 for $t_0 = 1$. This portion of the velocity profile is similar to that of the slow-heating case [11]. After the boundary-temperature rise cut-off at $t = t_0$, the piston-like action starts to decelerate as the velocity drops sharply and then more slowly as time goes on. This behavior is attributed to the decrease in the heat flux in the boundary-layer region after the cut-off time $t_0$.

The rate of heat flux at the wall is calculated to be

$$\dot{q} = k\frac{\partial T}{\partial x} = \epsilon^{-1/2}\left[2Ck\left(\frac{\Pr}{\pi}\right)^{1/2}\frac{t^{1/2}}{(1+Ct)}\right], \qquad t < t_0, \tag{56}$$

$$\dot{q} = \epsilon^{-1/2}\left\{2Ck\left(\frac{\Pr}{\pi}\right)^{1/2}\frac{t^{1/2}}{(1+Ct)}\left[1-(1-t_0/t)^{1/2}\right]\right\}, \qquad t \geqslant t_0. \tag{57}$$

The $O(\epsilon^{-1/2})$ rate of heat flux should be compared to the $O(\epsilon^{1/2})$ value found in [11].

The density and pressure fields in the boundary layer can be derived from the state equation and (36) respectively, along with (49)–(52). The pressure perturbation for $t < t_0$ is given by

$$\tilde{p}_0 = C\gamma\left[\left(\frac{4}{3}-\frac{1}{\Pr}\right)\left((1+2\eta^2)\,\mathrm{erfc}(\eta)-1\right)-\frac{2\eta}{\Pr\sqrt{\pi}}\right]+a(t), \tag{58}$$

where $a(t)$ is the constant of integration representing the value $\tilde{p}_0$ at the wall. It cannot be evaluated until the O($\epsilon$) core solution is found. The asymptotic properties of the functions appearing in (58) can be used to find the pressure at the edge of the boundary layer,

$$\tilde{p}_0(\eta \to \infty, t) = \frac{-2\gamma C}{\Pr\sqrt{\pi}}\eta + O(\eta^0). \tag{59}$$

The matching condition for the pressure in the core can be found by combining (10), the inverse of (15), (20), (29), (44) and (59) to produce

$$p(x \to 0, t) = 1 + \epsilon^{1/2}\left[\frac{-\gamma C}{\sqrt{\pi}\,\Pr}xt^{-1/2}\right] + O(\epsilon), \qquad t < t_0. \tag{60}$$

One may observe that the O($\epsilon^{1/2}$) correction is consistent with that used in the pressure transformation in (28). A similar result can be found for $t > t_0$.

*3d. The core solution*

The isentropic wave-propagation process in the interior region, representing the response of the core to the disturbance induced by the thermal expansion of the gas in the boundary layer, is described by (34) and (35). The appropriate boundary conditions are derived from the matching form of the boundary-layer solution (53) and (54) and are written as

$$x = 0, 1; \qquad \hat{u}_0 = \begin{cases} K_1 t^{1/2}, & t < t_0 \\ K_1\left[t^{1/2} - (t - t_0)^{1/2}\right], & t \geqslant t_0 \end{cases}, \tag{61}$$

where (28) has been used. Equations (34), (35) and (61) describe the isentropic dynamics of a gas in a confined region to which mass is added at a rapidly increasing rate when $t < t_0$, and at a decreasing rate when $t \geqslant t_0$.

A short-time, long-time and a general solution to (34) and (35) are derived in the Appendix. The general solution given in (A.12), is

$$\begin{aligned} \hat{u}_0(x, t) = {} & 2K_1\left(\tfrac{1}{2} - x\right)\left[t^{1/2} - (t - t_0)^{1/2}\mu(t - t_0)\right] \\ & - \frac{K_1}{2\pi}\sum_{m=1}^{\infty} m^{-3/2}\sin(2m\pi x)\left\{\cos(\xi_m)C_2(\xi_m) + \sin(\xi_m)S_2(\xi_m)\right. \\ & \left. - \mu(t - t_0)\left[\cos(\beta_m)C_2(\beta_m) + \sin(\beta_m)S_2(\beta_m)\right]\right\}, \end{aligned} \tag{62}$$

where $\xi_m = 2m\pi t$, $\beta_m = 2m\pi(t - t_0)$, $\mu(t - t_0)$ is the Heaviside step function and the functions $C_2$ and $S_2$ are Fresnel integrals [16]. This solution provides an analytical description of the kind of acoustic wave pattern, found numerically by Larkin [7], Thuraisamy [8] and Spradley et al. [9] for a slightly different initial-boundary value problem. The advantage of the analytical result for the present problem, where the temperature rise occurs over a well-defined time scale, is that the amplitude of the acoustic disturbance is specifically defined. In particular from (5), (10) and (28) one can observe that $u'/C_0' = O(\epsilon^{1/2})$, typically O($10^{-3}$) for standard conditions.

The density field can be obtained by integrating the conservation of mass equation (30) to yield

$$\hat{\rho}_0 = \tfrac{4}{3}K_1\left[t^{3/2} - (t-t_0)^{3/2}\mu(t-t_0)\right]$$
$$+\frac{K_1}{2\pi}\sum_{m=1}^{\infty} m^{-3/2}\cos(2m\pi x)\{\sin(\xi_m)C_2(\xi_m) - \cos(\xi_m)S_2(\xi_m)$$
$$-\mu(t-t_0)[\sin(\beta_m)C_2(\beta_m) - \cos(\beta_m)S_2(\beta_m)]\}. \tag{63}$$

The remaining field variables describing the isentropic process in the core, derived from (30)–(33), are given by

$$\hat{\rho}_0 = \gamma^{-1}\hat{p}_0 = (\gamma-1)^{-1}\hat{T}_0. \tag{64}$$

The purely time-dependent term in $\hat{\rho}_0$, $\hat{T}_0$ and $\hat{p}_0$ represents the accumulated adiabatic compression caused by the continuous succession of compression waves sweeping across the core. The series summations represent the spatial distribution of acoustic disturbances at an instant $t$. In the limit each term in the series in (62) reduces to the bounded form

$$m^{-3/2}\sin(2m\pi x)\left\{\sin\left[\xi_m + \frac{\pi}{4}\right] - \mu(t-t_0)\sin\left[\beta_m + \frac{\pi}{4}\right]\right\}. \tag{65}$$

The asymptotic properties of the Fresnel integrals $C_2$ and $S_2$ [16] have been used in deriving (65). It should be noted as well that the entire first term in the velocity (62) is $O(t^{-1/2})$ in the limit $t \to \infty$. In contrast the first purely time-dependent term in (63) is $O(t^{1/2})$ in the same limit.

One can observe from a combination of (28) and (62)–(64) that there are nonuniformities in the acoustic-time asymptotic expansions when $t = O(\epsilon^{-1})$. This condition corresponds to time measured with respect to the conduction time scale $t_c'$ defined at the beginning of Section 2. In this regard the conduction time variable is defined by

$$\tau = \epsilon t. \tag{66}$$

The asymptotic expansion of the variables show that on the conduction-time scale, when $\epsilon t = O(1)$, $\Delta T \sim \Delta p \sim \Delta\rho = O(1)$ and $u = O(\epsilon^{1/2})$. Of course on the conduction-time scale, the conceptual model consisting of a conductive boundary layer and a mechanically-responsive isentropic core fails to be a viable representation of reality. Rather a fully-conductive models must be constructed.

It is to be noted that the large $t$ estimates for the dependent variables can be used in a time-integrand form of the complete equation system (1)–(4) to show that nonlinear convection terms, neglected in the derivation of the acoustic equations in (30)–(33), have no accumulation effect on the linear acoustics when $t = O(\epsilon^{-1})$. In this respect nonlinear acoustic processes will not appear in the analysis.

## 4. Conduction-time solutions

The representation of the acoustic-time scale phenomena in the core during the earliest phase of the conduction-dominated process can be determined by developing the matching form of the variable expansions for $t \to \infty$. Equations (28), (29) and (62)–(64) can be combined appropriately in the limit $\epsilon \to 0$, $x$ fixed $(0 < x < 1)$ to obtain

$$u \sim -\epsilon^{1/2}\left[\frac{\sqrt{2}}{4\pi}K_1 \sum_{m=1}^{\infty} m^{-3/2}\sin(2m\pi x)\left\{\sin\left(\xi_m+\frac{\pi}{4}\right)-\sin\left(\beta_m+\frac{\pi}{4}\right)\right\}+\dots\right]$$

$$+\epsilon\left[K_1 t_0\left(\tfrac{1}{2}-x\right)\tau^{-1/2}+\dots\right]+\mathrm{O}(\epsilon^{3/2}), \tag{67}$$

$$\rho \sim 1+2K_1 t_0 \tau^{1/2}+\dots+\epsilon^{1/2}\left[\frac{\sqrt{2}}{4\pi}K_1 \sum_{m=1}^{\infty} m^{-3/2}\cos(2m\pi x)\right.$$

$$\left.\times\left\{\cos\left(\xi_m+\frac{\pi}{4}\right)-\cos\left(\beta_m+\frac{\pi}{4}\right)\right\}+\dots\right]+\mathrm{O}(\epsilon), \tag{68}$$

$$T \sim 1+2(\gamma-1)K_1 t_0 \tau^{1/2}+\dots+\epsilon^{1/2}\left[\frac{(\gamma-1)\sqrt{2}}{4\pi}K_1 \sum_{m=1}^{\infty} m^{-3/2}\right.$$

$$\left.\times\cos(2m\pi x)\cdot\left\{\cos\left(\xi_m+\frac{\pi}{4}\right)-\cos\left(\beta_m+\frac{\pi}{4}\right)\right\}+\dots\right]+\mathrm{O}(\epsilon), \tag{69}$$

$$p \sim 1+2\gamma K_1 t_0 \tau^{1/2}+\dots+\epsilon^{1/2}\left[\frac{\gamma\sqrt{2}}{4\pi}K_1 \sum_{m=1}^{\infty} m^{-3/2}\cos(2m\pi x)\right.$$

$$\left.\times\left\{\cos\left(\xi_m+\frac{\pi}{4}\right)-\cos\left(\beta_m+\frac{\pi}{4}\right)\right\}+\dots\right]+\mathrm{O}(\epsilon), \tag{70}$$

where $K_1$ is defined in (55) while $\xi_m$ and $\beta_m$ are given below (62). The asymptotic properties of Fresnel integrals [16] have been used in deriving these results. One may observe that the expressions for $\rho$, $T$ and $p$ contain an O(1)-term that varies with $\tau$ while the $\mathrm{O}(\epsilon^{1/2})$ term in $u$ describes a $t$-dependent field which represents the acoustic disturbance that continues to evolve on the conduction-time scale. The $\mathrm{O}(\epsilon)$-term in (67) represents the limiting form of the first term in (62). Since equations (68)–(70) are initial conditions for the long-time solution, the O(1) conduction-controlled process varying on the $\tau$-scale has superimposed upon it an $\mathrm{O}(\epsilon^{1/2})$ acoustic disturbance varying on the $t$-scale.

It should be pointed out that the core velocity and temperature results in (67) and (69) do not satisfy the boundary conditions given generally by (9). This implies that there exists an accommodation layer, occupying a thin region adjacent to the wall, in which the temperature is adjusted to the correct value. This accommodation layer is simply the conductive boundary layer as it evolves for $t \to \infty$. An expression for its structure can be written by using $\tau = \epsilon t$ in (50) and (52) and considering the limit $\tau \to 0$. It should be recalled that the boundary-layer solution given by (49)–(52) is obtained for the specific case when $\mu$ and $k$ are assumed to vary linearly with $\tilde{T}_0$. The O(1)-term in (69) satisfies a matching condition with the accommodation-layer solution for $x \to 0$.

Multiple time-scale analysis is suggested by the occurrence of simultaneous physical processes on both long conduction and short acoustic-time scales. The following transformations are implied by (67)–(70);

$$\begin{pmatrix}\rho\\ p\\ T\end{pmatrix}=\begin{pmatrix}\rho_c(\tau,x)\\ P_c(\tau,x)\\ T_c(\tau,x)\end{pmatrix}+\epsilon^{1/2}\begin{pmatrix}\rho_A(\tau,t,x)\\ p_A(\tau,t,x)\\ T_A(\tau,t,x)\end{pmatrix}+\epsilon\begin{pmatrix}\rho_2(\tau,t,x)\\ p_2(\tau,t,x)\\ T_2(\tau,t,x)\end{pmatrix}+\ldots, \tag{71}$$

$$u=\epsilon^{1/2}U_A(\tau,t,x)+\epsilon U_c(\tau,t,x)+\epsilon^{3/2}U_2(\tau,t,x)+\ldots, \tag{72}$$

where $\tau=\epsilon t$. The conduction-controlled and acoustic field variables are denoted by the subscripts $c$ and $A$ respectively. The time derivatives are written in a special form because $\tau$ and $t$ are treated as though they are independent variables. It follows that in (1), for instance,

$$\left(\frac{\partial\rho}{\partial t}\right)_x=\left(\frac{\partial\rho}{\partial t}\right)_{\tau,x}+\epsilon\left(\frac{\partial\rho}{\partial t}\right)_{t,x} \tag{73}$$

If (71)–(73) are used in (1)–(4) it is found that the equation system for the conduction-controlled field must be written initially in the form

$$\rho_{c_\tau}+(\rho_cU_c)_x=-\left\{\rho_{2_t}+(\rho_AU_A)_x\right\}, \tag{74}$$

$$P_{c_x}=0,\qquad P_c=\rho_cT_c, \tag{75}$$

$$\frac{C_v}{(\gamma-1)}\rho_c\left(T_{c_\tau}+U_cT_{c_x}\right)=-P_cU_{c_x}+\frac{\gamma}{(\gamma-1)\,\mathrm{Pr}}\left(k(T_c)T_{c_x}\right)_x$$
$$-\left\{\frac{C_v}{(\gamma-1)}\left[\rho_c\left(T_{2_t}+U_AT_{A_x}\right)+\rho_A\left(T_{A_t}+U_AT_{c_x}\right)\right]+P_AU_{A_x}\right\} \tag{76}$$

where $C_v$ has been treated as a constant. It is a characteristic of this multiple-time scale method that higher-order effects always appear in each approximation to the conservation of mass and energy equations. In this case the terms in (74) and (76) which are enclosed in brackets represent source terms which depend upon the variable $t$ and, in order that no secular terms appear in the conduction variables, these terms must be set equal to zero. The resulting equations provide formal constraints on $\rho_2$ and $T_2$ to within arbitrary functions of $\tau$ and $x$. The latter are found explicitly from the complete equation system for the third terms in (71) and (72).

The conduction-controlled process is then described by (75) and

$$\rho_c+(\rho_cU_c)_x=0, \tag{77}$$

$$\frac{C_v}{(\gamma-1)}\rho_c\left(T_{c_\tau}-U_cT_{c_x}\right)=-P_cU_{c_x}+\frac{\gamma}{(\gamma-1)\,\mathrm{Pr}}\left(k(T_c)T_{c_x}\right)_x \tag{78}$$

which are identical to the system used for the slow heating case in [11]. The appropriate initial conditions, obtained from (68)–(70), are

$$\tau = 0; \qquad \rho_c = T_c = p_c = 1, \qquad 0 < x < 1, \tag{79}$$

and the boundary conditions are given by

$$x = 0, 1; \qquad u_c = 0, \qquad T_c = 1 + Ct_0, \qquad \tau > 0. \tag{80}$$

The conditions on $T_c$ represent an impulsive increase in the boundary temperature by the amount $Ct_0$.

The acoustic field equations are found to be

$$\rho_{A_t} + (\rho_c U_A)_x = 0, \qquad p_A = \rho_A T_c + \rho_c T_A, \tag{81}$$

$$\gamma \rho_c U_{A_t} + p_{A_x} = 0, \tag{82}$$

$$\frac{C_v}{(\gamma - 1)} \rho_c \left[ T_{A_t} + U_A T_{c_x} \right] = -p_c U_{A_x}. \tag{83}$$

The appropriate boundary and initial conditions are

$$x = 0, 1; \qquad U_A = 0, \qquad T_A = 0, \tag{84}$$

$$\tau \to 0; \qquad U_A = -\frac{\sqrt{2}}{4\pi} K_1 \sum_{m=1}^{\infty} m^{-3/2} \sin(2m\pi x) \left\{ \sin\left( \xi_m + \frac{\pi}{4} \right) - \sin\left( \beta_m + \frac{\pi}{4} \right) \right\}, \tag{85}$$

$$\tau \to 0; \qquad \rho_A = p_A/\gamma = T_A/(\gamma - 1) = -K_1 \frac{(2)^{-3/2}}{\pi} \sum_{m=1}^{\infty} m^{-3/2} \cos(2m\pi x) \times \left\{ \cos\left( \xi_m + \frac{\pi}{4} \right) - \cos\left( \beta_m + \frac{\pi}{4} \right) \right\}, \tag{86}$$

where (85) and (86) are obtained from (67)–(70). It should be noted that these initial conditions are a corrected form of those given in [11] for the analogous slow-heating case. In mathematical terms, when $0 < \tau \ll 1$, $t$ can be arbitrarily large. It follows that $\xi_m$ and $\beta_m$ may be large. Kassoy [11] ignored this point and set $\xi_m = 0$. Equations (85) and (86) imply that, from the viewpoint of conduction-time-scale processes, the acoustic field has existed for a long time. It follows that the acoustic frequencies found for $\tau \to 0$ are determined by those found in the ancestral acoustic field evolving in the isentropic core.

The first of (75) can be interpreted to mean that the pressure rise for the long-time process is spatially homogeneous. Multiple reflections of acoustic waves within the slot over the time $\tau = O(1)$ produce this effect. A specific expression for $P_c(\tau)$ can be obtained by integrating the mass-conservation equation (77) across the slot and using (80) and (84) along with the second of (75). It follows that

$$P_c(\tau) = \left[ \int_0^1 \frac{dx}{T_c(\tau, x)} \right]^{-1} \tag{87}$$

which was also found in the case of slow wall heating [11]. This statement means that the pressure at any time is inversely proportional to the averaged inverse temperature.

A considerable simplification of the conduction-controlled system is found if the Lagrangian variable

$$y=\int_0^x \rho_c(\tau, s)\mathrm{d}s \tag{88}$$

is employed in (77), (78) and (87). The result

$$\rho_{c_\tau}+\rho_c^2 U_{c_y}=0, \tag{89}$$

$$T_{c_\tau}=\frac{P_c}{\mathrm{Pr}} T_{c_{yy}}+\frac{(\gamma-1)}{\gamma} \frac{T_c}{P_c} P_{c_\tau}, \tag{90}$$

$$P_c(\tau)=\int_0^1 T_c(\tau, y)\mathrm{d}y, \tag{91}$$

is valid for $C_v=1$. The last term in (90) represents the effect of compressive heating arising from the pressure increase in a constant volume system described by (91). In a system with boundary heat addition where $P_{c_\tau}>0$, the last term in (90) acts as an effective heat source. These equations, along with the second of (75), (79) and (80) define a typical initial-boundary value problem. Once $T_c$ is computed numerically from the integro-differential equation constructed from (90) and (91), the pressure $P_c$ and the density $\rho_c$ are found from (91) and (75) respectively. An explicit expression for the velocity field, obtained from an integral of (89) and the condition at $x=0$ ($y=0$) in (80),

$$U_c(\tau, y)=-\frac{\partial}{\partial \tau} \int_0^y \frac{T_c(\tau, s)\mathrm{d}s}{P_c(\tau)}, \tag{92}$$

also satisfies the condition at $x=1$, ($y=1$) automatically given the result in (91). Detailed numerical solutions are described in Section 5.

The completed conduction-controlled solution can then be used in (81)–(86) which describes the linear propagation of acoustic waves in a slowly-varying inhomogeneous medium contained in a finite space. When $C_v=1$ these equations can be rearranged to show that

$$U_{A_{tt}}=T_c(\tau, x)U_{A_{xx}}. \tag{93}$$

The boundary and initial conditions in (84) and (85) must be satisfied. It is essential to note that the latter is a condition for $\tau \rightarrow 0$ and not for $t \rightarrow 0$. The general solution can be written as the real part of

$$U_A=\sum_{m=1}^{\infty} i g_m(x; \tau)\left[\exp(i\sigma_m)-\exp(i[\sigma_m-2m\pi t_0])\right],$$

$$\sigma_m=\lambda_m(\tau)t+\frac{\pi}{4}, \tag{94}$$

such that

$$g_m(x;0) = \frac{\sqrt{2}\,K_1}{4\pi} m^{-3/2} \sin 2m\pi x, \qquad \lambda_m(0) = 2m\pi. \tag{95}$$

The amplitude equation is given by

$$T_c(\tau, x) g_m''(x;\tau) + \lambda_m^2(\tau) g_m = 0, \qquad g_m(0;\tau) = g_m(1;\tau) = 0 \tag{96}$$

where primes denote derivatives with respect to $x$. Clearly (95) is a solution when $\tau \to 0$ because $T_c \to 1$. In fact (95) sets the absolute magnitude of the amplitude function. The general properties of this self-adjoint eigenvalue problem are of some interest because they could be used to determine how the amplitude varies with the parameter $\tau$ in a given $T_c(\tau, x)$. In the case of boundary heating, $T_c(\tau, x) \geqslant 1$ and $T_{c_\tau}(\tau, x) > 0$ for $0 < x < 1$, it would be desirable to know how each eigenfunction varies with $\tau$ at any specified $x$ location. Unfortunately general theorems do not appear to be available, although Sturm-Liouville theory [18] can be used to show that $\lambda_m(\tau)$ increases with $\tau$ when $T_{c_\tau} > 0$. Some indication of solution properties can be obtained for special $T_c$-distributions. In the case of a background temperature $T_c = \alpha(\tau)\mathrm{h}(x)$ which increases everywhere at the same rate (96) can be reduced to

$$h(x) g_m''(x) + \Omega_m^2 g_m = 0, \qquad g_m(0) = g_m(1) = 0, \tag{97}$$

for $\lambda_m^2(\tau) = \Omega_m^2 \alpha(\tau)$ where $\Omega_m$ is a constant and $g_m$ depends only on $x$. It follows that the eigenvalue is independent of $\tau$, although the slowly-varying wave number is not. Unfortunately (94) cannot be satisfied for nontrivial $h(x)$. This occurs because the assumed form for $T_c$ is not an admissible solution to the conduction-controlled system. However the result suggests that eigenvalue variation with $\tau$ will require a spatially dependent temperature rise rate. In the case of $T_c = k^2(\tau)(A(\tau) - x)^2$, $A > 1$ the transformation

$$S = k^{-1} \ln\left(\frac{A}{A - x}\right)$$

can be used to convert (96) to

$$g_m''(s;\tau) + k(\tau) g_m' + \lambda_m^2 g_m = 0$$

where primes denotes derivatives with respect to $s$. The solution which satisfies the boundary conditions in (96) can be written in terms of $x$ as

$$g_m(x;\tau) = \left(\frac{A - x}{A}\right)^{1/2} \sin\left( m\pi \frac{\ln\left(\dfrac{A}{A - x}\right)}{\ln\left(\dfrac{A}{A - 1}\right)} \right), \tag{98}$$

$$\lambda_m^2 = \frac{k^2}{4}\left[1 + \frac{4m^2\pi^2}{\ln[A/(A - 1)]}\right].$$

If $A_\tau > 0$ then the eigenfunction increases (decreases) with $\tau$ when the sine function is positive (negative). The wave number $\lambda_m$ is an increasing function of $\tau$. This type of behavior occurs for a spatially-dependent rate of temperature increase defined by $T_c$. Here again the result in (98) cannot satisfy (95) because $T_c$ does not have the correct behavior for $\tau \to 0$ ($T_c \to 1$). Nevertheless the results show that for a fairly general background-temperature distribution, not unlike that which might be found in a conduction-dominated process, amplitude variation can occur.

Perhaps the best estimate of eigenfunction behavior, short of a full numerical calculation, can be obtained for a large-wave-number approximation to (96). A multiple-variable method [20] related to the WKB-approximation can be employed for $m \gg 1$ to find

$$g_m(x, \xi_m; \tau) = \frac{\sqrt{2}\, K_1}{4\pi m^{3/2}} T_c^{1/2}(\tau, x) \sin \xi_m + \mathrm{O}(m^{-5/2}), \tag{99a}$$

$$\lambda_m = 2m\pi \left[ \int_0^1 \frac{\mathrm{d}\tau}{T_c^{1/2}} \right]^{-1}, \tag{99b}$$

$$\xi_m(x) = \lambda_m \int_0^x \frac{\mathrm{d}\tau}{T_c^{1/2}}, \tag{99c}$$

where $x$ and $\xi_m$ are treated as independent variables. Here for $T_{c_\tau} > 0$, $0 < x < 1$, the eigenfunction increases (decreases) with $\tau$ when the sine function is positive (negative). The wave number $\lambda_m$ is explicitly increasing with $\tau$. Equation (95) has been satisfied to obtain a specific amplitude! Equation (99) can be used to show that each of the large-wave-number modes of $U_A$ can be written as a linear superposition of four travelling waves. The amplitude of each of these waves increases with $\tau$ like $[T_c(\tau, x)]^{1/2}$.

Once $U_A$ is found, the remaining acoustic variables can be obtained from (81)–(83). For example the acoustic pressure field is given by the real part of

$$p_A = -\gamma P_c(\tau) \sum_{m=1}^{\infty} \left[ \frac{g_{m_x}(x; \tau)}{\lambda_{m(\tau)}} \right] [\mathrm{e}^{i(\lambda_m t + \pi/4)} - \mathrm{e}^{i(\lambda_m + \pi/4 - 2m\pi t_0)}]. \tag{100}$$

The large-wave-number modes of (100) can be written in a first approximation as

$$-\frac{2^{1/2} K_1 \gamma}{4\pi} P_c(\tau) \frac{\cos \xi_m}{m^{3/2}} \left( \cos\left(\lambda_m t + \frac{\pi}{4}\right) - \cos\left(\lambda_m t + \frac{\pi}{4} - 2m\pi t_0\right)\right) \tag{101}$$

given the results in (99). Once again these modes can be split into four travelling waves with amplitudes that increase like $P_c(\tau)$.

It should be noted that the wall boundary condition for (83) given in the last of (84) cannot be satisfied because $U_{A_x}(\tau, t, 0) \neq 0$. This difficulty arises because of the absence of conductive heat transfer in (84) which would allow for accommodation of the acoustic temperature field with that at the wall. Rott [13] has described the structure of such layers in detail.

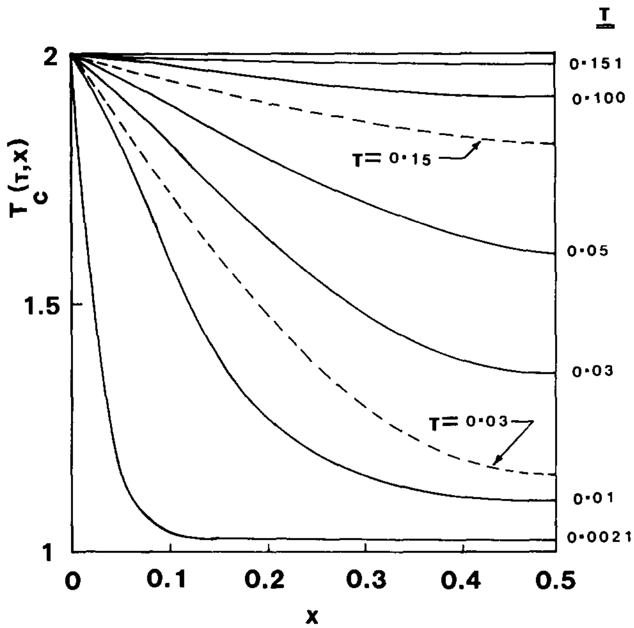


Figure 3. The variation of the spatially-dependent temperature $T_c$ with the conduction-time variable $\tau$ when $Ct_0 = 1$, $\gamma = 1.4$ and $Pr = 1$. Dashed lines correspond to a rigid-material temperature.

## 5. Numerical results

A numerical solution of the integrodifferential equation for $T_c$, obtained from (90) and (91), subject to the initial and boundary conditions in (79) and (80) has been developed by using the method of lines [19]. Details of the procedures employed can be found in

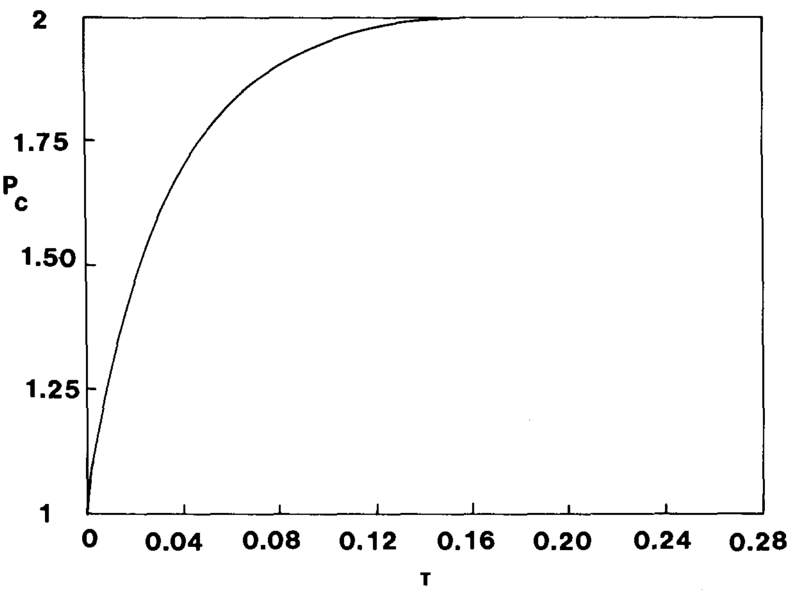


Figure 4. The variation of the spatially-homogeneous pressure $P_c$ with the conduction-time variable $\tau$ when $Ct_0 = 1$, $\gamma = 1.4$ and $Pr = 1$.

Radhwan [12]. In Fig. 3 the spatial temperature distribution is shown as a function of the condition time variable $\tau$ when $Ct_0 = 1$, $\gamma = 1.4$ and $\mathrm{Pr} = 1$. The inverse of the Lagrangian transformation in (88) has been used to produce results in the physical variable $x$. Only half the slab is depicted because the basic problem is symmetric. For $\tau \ll 0.01$ the temperature field has a boundary-layer structure near the wall. The spatially homogeneous temperature rise in the core for small $\tau$ due to compression, is in very close agreement with the first two terms in (69). When $\tau \approx 0.15$ the temperature has almost reached the final equilibrium value.

The effect of gas motion on the heat-transfer process is to accelerate the approach to equilibrium. This can be seen in Fig. 3 where the temperature profiles for an equivalent rigid material [15] are shown for $\tau = 0.03$ and 0.15. These profiles lag behind the analogous gas solutions by a substantial amount. The enhancement of heat transfer arises from convention of energy by the small ($10^{-6}$) $U_c$-field. Larkin [7] and Spradley et al. [9] observed very similar effects in their related problem.

The spatially-homogeneous pressure rise, given in Fig. 4, is found from (91). The early increase is predicted almost exactly by the $\tau$-dependent terms in (70). The approach to the

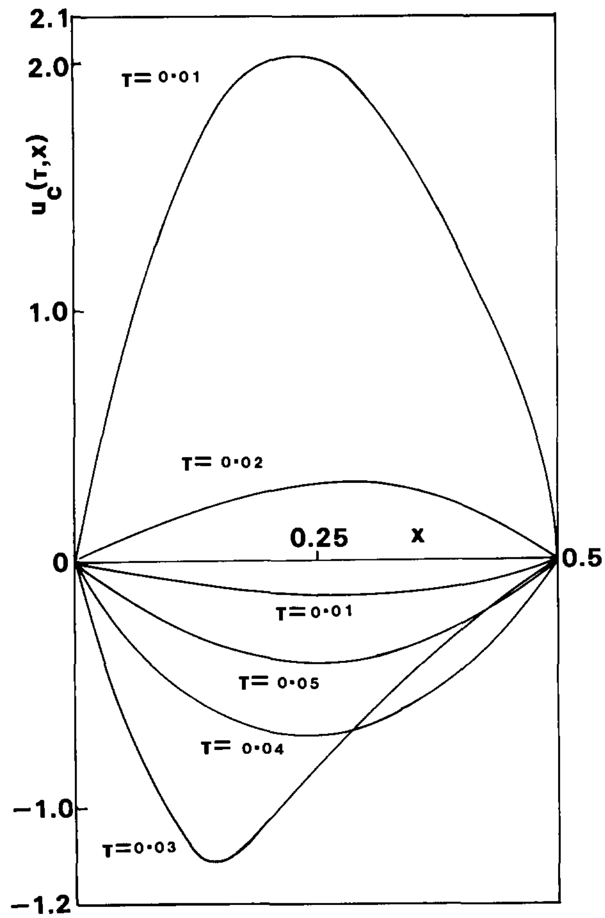


Figure 5. The variation of the spatially-dependent velocity with the conduction-time variable $\tau$ when $Ct_0 = 1$, $\gamma = 1.4$ and $\mathrm{Pr} = 1$.

final equilibrium state occurs when the temperature distribution in Fig. 3 is nearly spatially uniform.

The velocity distribution driven by thermal expansion is shown in Fig. 5. For sufficiently short times the boundary-layer structure is apparent. The maximum lies near the heated boundary. Beyond the boundary layer the velocity decays like the $O(\epsilon)$ term in the core solution in (67). Until about $\tau = 0.02$ mass is moved toward the centerline. The location of the velocity maximum moves to the right as the magnitude decreases. Eventually flow reversal develops as the displaced mass moves back toward the wall.

## 6. Conclusions

The physical consequences of the mathematical modelling can be considered by applying the results to a typical inert gas. If we assume that the slab is filled with air at $P_0' = 1$ atm, $T_0' = 25°C$ and that $L' = 10$ cm, then the acoustic and conduction times are $t_A' = 3.01 \times 10^{-4}$ s and $t_0' = 442$ s respectively. For $\Pr = 0.76$ the small parameter $\epsilon = 4.77 \times 10^{-7}$.

During the acoustic time period, when the wall temperature increase by a significant factor relative to the absolute initial value, the conduction boundary-layer thickness is about $7 \times 10^{-3}$ cm. The power added to that gas layer is characterised by $10^7$ W/m$^2$. Gas expansion in the boundary layer, arising from the temperature rise induces a maximum speed of about 20 cm/s. The resulting mechanical disturbance at the boundary-layer edge causes the continuous generation of compressive acoustic waves in the core of the slab. Eventually these accumulate into a bulk velocity distribution with a maximum value of about 20 cm/s and a spatially-homogeneous compression perturbation which is typically $10^{-3}\, P_0'$.

Further evolution of the heat-transfer process on the conduction-time scale is associated with significant spatial variation of temperature and density. The associated major pressure increase is spatially homogeneous because a weak acoustic field is able to smooth disturbances during the long conduction time period. As long as the finite boundary-temperature increase occurs entirely during the acoustic-time period, the primary velocity field is that evolving from the previously-generated acoustic field which is characterised by a speed of 20 cm/s. The acoustic waves now move through an inhomogeneous slowly-varying background. As a result the generalised Fourier-decomposition of the evolving acoustic field is characterised by slowly-varying amplitudes and wave numbers. The speed associated with the much weaker bulk gas deformation process is typically $1.5 \times 10^{-2}$ cm/s. This slowly-varying field displays flow reversal resulting from the need to conserve mass in a variable density field.

A heat-addition rate of substantial magnitude occurs briefly at the boundary. The power added, typically $10^3$ W/m$^2$ generates an effective piston Mach number (see for example (47)) of only $10^{-3}$. This value is sufficiently small to assure that the linear wave front generated initially in the core cannot become nonlinear within the container during the time periods of interest. This shows in a quantitative manner in the context of a finite system that a more substantial energy pulse is necessary to generate weak shocks in a finite container. For the heat-addition mechanism considered in the present work (conduction) sharper pulses are required. This effect will be discussed in a subsequent paper [21].

The amplitude of the acoustic pressure field initiated early in the process and which continues to evolve throughout the events is $O(10^{-3})$. The corresponding intensity is a factor of $10^3$ larger than the standard intensity of $I_0 = 1$ $\mu$W/cm$^2$ Normal speech levels are associated with $10I_0$. In this regard one should recognize that rapid boundary heating of a compressible gas, or for that matter an equivalent localised heat release due to combustion, can be effective source of rather painful levels of noise generation.

## Appendix

Laplace-transform methods were employed to find the solution to (34), (35) and (61). The transformed solution is obtained for $0 \leqslant x \leqslant \frac{1}{2}$ as

$$U(x, s) = L[\hat{u}_0] = K_2 \frac{(1 - e^{-t_0 s}) \sinh(\frac{1}{2} - x)s}{s^{3/2} \sinh(s/2)} \tag{A.1}$$

where

$$K_2 = \frac{K_1 \pi^{1/2}}{2}.$$

The symmetry property of the problem has been exploited in obtaining (A.1) where the velocity is assumed to vanish at the mid-plane ($x = \frac{1}{2}$). The short-time ($s \to \infty$) transform is given by

$$U(s, x) \sim K_2 s^{-3/2} e^{-sx} \tag{A.2}$$

and can be inverted [16] to give

$$\hat{u}_0(x, t) = K_1 (t - x)^{1/2}, \qquad 0 < t < \tfrac{1}{2}. \tag{A.3}$$

A solution for large times, obtained from the inversion of the long-time transform ($s \to 0$),

$$U(x, s) \sim 2K_2 t_0 (\tfrac{1}{2} - x) s^{-1/2} + O(S^{1/2}), \tag{A.4}$$

is

$$\lim_{t \to \infty} \hat{u}_0(x, t) \sim K_1 t_0 (\tfrac{1}{2} - x) t^{-1/2} + \cdots. \tag{A.5}$$

To find the general solution one can write (A.1) as

$$U(x, s) = K_2 \frac{\sinh(\frac{1}{2} - x)s}{s^{3/2} \sinh(s/2)} - K_2 \frac{\sinh(\frac{1}{2} - x)s}{s^{3/2} \sinh(s/2)} e^{-t_0 s}. \tag{A.6}$$

The first term can be written as

$$\hat{F} = K_1 \hat{f}_1(s) \hat{f}_2(s) \tag{A.7}$$

where

$$\hat{f}_1(s) = s^{-1/2}, \qquad \hat{f}_2(s) = \frac{\sinh(\frac{1}{2} - x)s}{s \sinh(s/2)}. \tag{A.8}$$

The Laplace inverse of $\hat{f}_1(s)$ is

$$L^{-1}[\hat{f}_1(s)] = 1/\sqrt{\pi t}. \tag{A.9}$$

The function $\hat{f}_2(s)$, inverted by using the residue theorem [17], is given by

$$f_2(t) = 2(\tfrac{1}{2} - x) + \sum_{m=1}^{\infty} \frac{(-1)^m}{m\pi} \sin[2m\pi(\tfrac{1}{2} - x)] \cos(2m\pi t). \tag{A.10}$$

The convolution theorem is used to obtain the inverse of the function $\hat{F}$ in the form

$$F(x, t) = 2K_1(\tfrac{1}{2} - x)t^{1/2} - \frac{K_1}{2\pi} \sum_{m=1}^{\infty} m^{-3/2} \sin(2m\pi x)$$
$$\times [\cos(\xi_m)C_2(\xi_m) + \sin(\xi_m)S_2(\xi_m)] \tag{A.11}$$

where $\xi_m = 2m\pi t$ and the functions $C_2$ and $S_2$ represent Fresnel integrals [16]. The Laplace inverse of the second term (A.6) is the same as (A.11) except that $t$ is shifted by $t_0$. Collecting the Laplace inverse of those functions, one can write the inverse of (A.1) as

$$\hat{u}_0(x, t) = 2K_1(\tfrac{1}{2} - x)[t^{1/2} - (t - t_0)^{1/2}\mu(t - t_0)]$$
$$- \frac{K_1}{2\pi} \sum_{m=1}^{\infty} m^{-3/2} \sin(2m\pi x)\{\cos(\xi_m)C_2(\xi_m) + \sin(\xi_m)S_2(\xi_m)$$
$$- \mu(t - t_0)[\cos(\beta_m)C_2(\beta_m) + \sin(\beta_m)S_2(\beta_m)]\} \tag{A.12}$$

where $\beta_m = 2m\pi(t - t_0)$ and $\mu(t - t_0)$ is the Heaviside step function.

## Acknowledgement

This work was completed whilst D.R.K. was a Senior Visiting Fellow supported by the UK Science and Engineering Research Council at the University of East Anglia. Additional support was provided by a contract from the US Army Research Office DAAG29-84-K-0069, and by a Faculty Fellowship from the University of Colorado.

## References

[1] Lord Rayleigh, On the conduction of heat in a spherical mass of air confined by walls at a constant temperature, *Phil. Mag.* XLVII (1899) 314–325.
[2] T.Y. Wu, Small perturbations in the unsteady flow of a compressible, viscous and heat conducting fluid, *J. Math. Phys.* 35 (1956) 13–27.
[3] L. Trilling, On thermally induced sound fields, *J. Acoustical Soc. Am.* 27 (1955) 425–431.
[4] J.R. Knudsen, The effects of viscosity and heat conductivity on the transmission of plane sound waves, *J. Acoust. Soc. Am* 26 (1957) 51–57.
[5] A.V. Luikov and B.M. Berkoresky, Thermoconvective waves, *Int. J. Heat Mass Transfer* 13 (1970) 741–747.

[6] B.T. Chu, Pressure waves generated by addition of heat in a gaseous medium, NACA-TN 3411 (1955), National Advisory Committee for Aeronautics, Washington D.C.

[7] B.K. Larkin, Heat flow to a confined fluid in zero gravity, *Progress in Astronautics and Aeronautics, Thermophysics of Space and Planetary Bodies*, ed. G.B. Heller, 30 (1967) 819–832.

[8] V. Thuraisamy, Thermodynamic flow of supercritical oxygen in zero-gravity, *Bellcomm.* TM-72-1022-1, (1972) Bellcomm. Inc., Washington, D.C.

[9] L.W. Spradley, S.V. Bourgeois, C. Fan and P.G. Grodzka, A numerical solution for thermoacoustic convection of of fluids in low gravity, *NASA Contractor Rept.* CR-2269, (1973) NASA, Washington, D.C.

[10] L.W. Spradley and S.W. Churchill, Pressure and buoyancy driven thermal convection in a rectangular enclosure, *J. Fluid Mech.* 70 (1975) 705–720.

[11] D.R. Kassoy, The response of a confined gas to a thermal disturbance: Slow transients, *SIAM J. Appl. Math.* 36 (1979) 624–634.

[12] A.M. Radhwan, The mechanical response of a gas to boundary heat addition, Ph.D. Thesis, The University of Colorado (1981), Boulder, Colorado.

[13] N. Rott, Thermoacoustics, *Adv. in Appl. Mech.* 20 (1980) pp. 135–174.

[14] W.G. Vincenti and S.C. Traugott, The coupling of radiative transfer and gas motion, *Ann. Rev. Fluid Mech.* 3 (1971) 89–116.

[15] H.S. Carslaw and J.C. Jaeger, *Conduction of heat in solids*, 2nd edn. (1978) Oxford University Press, Oxford, England.

[16] M. Abramowitz and I. Stegun, *Handbook of mathematical functions*, National Bureau of Standards (1965), Washington D.C.

[17] R.V. Churchill, *Operational mathematics*, 2nd edn. (1958), McGraw-Hill Book Co., New York.

[18] E.L. Ince, *Ordinary differential equations*, (1956), Dover Publications, New York.

[19] R.L. Ketter and S.P. Prawel, *Modern methods of engineering computation*, (1969), McGraw-Hill Book Co., New York.

[20] J.D. Cole, *Perturbation methods in applied mathematics*, (1968), Blaisdell Pub. Co., Waltham, Mass.

[21] J.F. Clarke, D.R. Kassoy and N. Riley, Weak shock generation in a confined gas due to rapid heat addition at the boundary, to appear in *Proc. Royal Soc.* A (1984).